This is the post peer-review accepted manuscript of:

A. Giorgetti, K. Magowe, S. Kandeepan, "Exact analysis of weighted centroid localization," European Signal Processing Conference (EUSIPCO), pp. 743-747, Budapest, Aug. 2016.

The published version is available online at:

https://doi.org/10.1109/EUSIPCO.2016.7760347

Exact Analysis of Weighted Centroid Localization

Andrea Giorgetti*, Kagiso Magowe†, and Sithamparanathan Kandeepan†

*DEI, University of Bologna, Italy
†School of Engineering, RMIT University, Melbourne, Australia
Email:{a.giorgetti, kagiso.magowe.au, sithamparanathan.kandeepan}@ieee.org

***Abstract*—Source localization of primary users (PUs) is a geolocation spectrum awareness feature that can be very useful in enhancing the functionality of cognitive radios (CRs). When the cooperating CRs have limited information about the PU, weighted centroid localization (WCL) based on received signal strength (RSS) measurements represents an attractive low-complexity solution. In this paper, we propose a new analytical framework to calculate the exact performance of WCL in the presence of shadowing, based on results of the ratio of two quadratic forms in normal variables. In particular, we derive an exact expression for the root mean square error (RMSE) of the two-dimensional location estimate. Numerical results confirm that the derived framework is able to predict the performance of WCL capturing all the essential aspects of propagation as well as CR network spatial topology.**

I. Introduction

The wireless communication area has seen the introduction of new paradigms that aim to combat the issue of radio frequency spectrum scarcity. Cognitive radio (CR) is one of the emerging technologies that has been developed and studied over the past decade to enable efficient utilization of the spectrum resources [1]. In CR networks, spectrum sensing is a key enabler in identifying spectrum holes and monitoring of the primary user (PU) activity so as to avoid any potential harmful interference [2].

However, it should be noted that sensing functionality includes any kind of technique that allows the CRs to gather useful radio environment information and enhance the functionality of the network. Therefore, geo-location of PU is one such spectrum awareness technique that not only plays an important role in preventing harmful interference to the PU, but allows for better spectrum resource allocations in the spatial domain [3]–[9]. Bearing in mind the challenges posed by the uncooperative nature of the PU, weighted centroid localization (WCL) represents an attractive low complexity solution which relies only on received signal strength (RSS) measurements.

The WCL technique has been studied in several papers assuming the secondary users (SUs) have limited information about the PU [10]–[14]. Most of them evaluate the WCL performance in terms of the root mean square error (RMSE) only numerically, under varying environment conditions i.e., factors such as node placement, node density, shadowing variance and node spacing. For instance, the work in [11] analysed the WCL performance under varying path-loss exponent, different weighting strategies, node selection strategy and further explored the dependence of the RMSE on the position of the PU within the area considered. In [12], we investigated the WCL performance when adopting a geometric based node selection strategy i.e., imposing a geometric constraint to the selection of SUs. The first theoretical framework for WCL analysis using a probabilistic approach was presented in [14], assuming that the two-dimensional localization errors are jointly Gaussian, thus requiring the calculation of the error covariance matrix.

In this paper, we propose a new analytical framework to calculate the exact performance of WCL in the presence of independent and identically distributed (i.i.d.) log-normal shadowing, based on results of the ratio of two quadratic forms in normal variables [15]–[17]. In particular, the main results of this paper can be summarized as follows:

- We derive the expression for the RMSE of the two-dimensional location estimation.
- The exact expression is based on the statistical distribution of the ratio of quadratic forms in normal variables.
- Through the new analytical methodology we quantify the performance of WCL in different scenarios by varying the PU locations, the path-loss exponent, the number of SUs and their location.

The remainder of this paper is organized as follows. In Section II we present the system model. The new theoretical framework that leads to the derivation of the exact calculation of the RMSE is provided in Section III. In Section IV we analyze a case study to quantify the effectiveness of the proposed approach. Section V concludes the paper. For the sake of conciseness, Table I summarizes the notations and symbols used.

TABLE I
Notations and Symbols

X	Random variable
$\mathbf{X}$	Random vector or matrix
x	Realization of a random variable
$\mathbb{E}[\cdot]$	Expectation operator
$\mathrm{Tr}(\cdot)$	Trace operator
$\det(\cdot)$	Determinant of a matrix
$\mathrm{diag}(\cdot)$	Diagonal matrix
$\mathbf{I}$	Identity matrix
$\mathbf{1}$	Matrix of ones
$[\cdot]^{\mathrm{T}}$	Transpose operator
$\|\|\cdot\|\|_l$	l-th norm operator
$\mathcal{N}(\mu,\sigma^2)$	Gaussian distribution with mean μ and variance σ^2

II. System Model

We consider a CR network with N SUs located in a square area of side length $\mathcal{S}$, and the PU located within the area at position $\mathbf{L}_{\mathrm{p}} = [x_{\mathrm{p}}, y_{\mathrm{p}}]^{\mathrm{T}}$. The position of the i-th SU node is defined as $\mathbf{L}_i = [x_i, y_i]^{\mathrm{T}}$, $i = 1, 2, ..., N$. The propagation environment is characterized by a power-law path-loss channel model plus log-normal shadowing. The RSS at the i-th SU node from the PU is thus given by

$$P_i = P_{\mathrm{t}} - p_{\mathrm{l}}(d_0) - 10\,\alpha \log_{10}\left(\frac{||\mathbf{L}_i - \mathbf{L}_{\mathrm{p}}||_2}{d_0}\right) + S_i \qquad (1)$$

where P_{t} is the transmit power in dBm, $p_{\mathrm{l}}(d_0)$ is the path-loss at a reference distance d_0, α is the path-loss exponent, and $S_i \sim \mathcal{N}(0, \sigma_{\mathrm{s}}^2)$ describes the random shadowing effect.

We begin by presenting the WCL algorithm used to estimate the location of the PU in two dimensions [10]

$$\widehat{\mathbf{L}}_{\mathrm{p}} = \frac{\sum_{i=1}^{N} w_i \mathbf{L}_i}{\sum_{i=1}^{N} w_i} = \frac{\sum_{i=1}^{N} (P_i - P_{\min})\mathbf{L}_i}{\sum_{i=1}^{N} (P_i - P_{\min})} \qquad (2)$$

where $w_i = (P_i - P_{\min})/(P_{\max} - P_{\min})$ is the weighting coefficient for the i-th SU node, with $P_{\max}$ the maximum received power among sensor nodes, and $P_{\min}$ an arbitrary reference power level which can be e.g., the minimum measurable received power by the SU. The localization error is defined as $\boldsymbol{\xi} \triangleq \widehat{\mathbf{L}}_{\mathrm{p}} - \mathbf{L}_{\mathrm{p}} = [\widehat{X}_{\mathrm{p}} - x_{\mathrm{p}}, \widehat{Y}_{\mathrm{p}} - y_{\mathrm{p}}]^{\mathrm{T}}$, where $\widehat{X}_p$ and $\widehat{Y}_p$ are the one-dimensional position estimates along the x-axis and y-axis, respectively

$$\widehat{X}_p = \frac{\sum_{i=1}^{N} G_i x_i}{\sum_{i=1}^{N} G_i} \qquad \widehat{Y}_p = \frac{\sum_{j=1}^{N} G_j y_j}{\sum_{j=1}^{N} G_j} \qquad (3)$$

with $G_i = P_i - P_{\min}$. Finally, the distance error is given by

$$\xi \triangleq \sqrt{(\widehat{X}_{\mathrm{p}} - x_{\mathrm{p}})^2 + (\widehat{Y}_{\mathrm{p}} - y_{\mathrm{p}})^2} = ||\boldsymbol{\xi}||_2. \qquad (4)$$

For notational convenience we define $\mathbf{G} = [G_1, \ldots, G_N]^{\mathrm{T}}$, $\mathbf{X} = [x_1, \ldots, x_N]^{\mathrm{T}}$, and $\mathbf{Y} = [y_1, \ldots, y_N]^{\mathrm{T}}$. In the following section, the square of the distance error (4) will be interpreted as the ratio of two quadratic forms, leading to a new theoretical framework for the performance analysis of WCL.

III. Exact Calculation of the Root Mean Square Error

In this section we derive an exact expression of the RMSE of the two-dimensional location estimate. Defining $\xi_{\mathrm{x}} = \widehat{X}_{\mathrm{p}} - x_{\mathrm{p}}$ and $\xi_{\mathrm{y}} = \widehat{Y}_{\mathrm{p}} - y_{\mathrm{p}}$ as the errors in the x-dimension and y-dimension, respectively, the RMSE can be written as

$$\begin{aligned}\mathsf{RMSE} = \sqrt{\mathsf{MSE}} &= \sqrt{\mathbb{E}\left[||\widehat{\mathbf{L}}_{\mathrm{p}} - \mathbf{L}_{\mathrm{p}}||_2^2\right]} \\ &= \sqrt{\mathbb{E}\left[\xi_{\mathrm{x}}^2 + \xi_{\mathrm{y}}^2\right]}. \end{aligned} \qquad (5)$$

The argument of the expectation in (5) can be rewritten as

$$\begin{aligned}\xi^2 &= \xi_{\mathrm{x}}^2 + \xi_{\mathrm{y}}^2 \\ &= \left(\frac{\sum_{i=1}^{N} G_i(x_i - x_{\mathrm{p}})}{\sum_{i=1}^{N} G_i}\right)^2 + \left(\frac{\sum_{i=1}^{N} G_j(y_j - y_{\mathrm{p}})}{\sum_{i=1}^{N} G_j}\right)^2 \\ &= \frac{\sum_{i=1}^{N}\sum_{j=1}^{N} G_i G_j a_{ij}}{\sum_{i=1}^{N}\sum_{j=1}^{N} G_i G_j}\end{aligned}$$

where $a_{ij} = (x_i - x_{\mathrm{p}})(x_j - x_{\mathrm{p}}) + (y_i - y_{\mathrm{p}})(y_j - y_{\mathrm{p}})$. Defining $x_i' = x_i - x_{\mathrm{p}}$ and $y_i' = y_i - y_{\mathrm{p}}$, the term a_{ij} can be expressed as $a_{ij} = x_i' x_j' + y_i' y_j'$, and arranged in a matrix form $\mathbf{A} = [a_{i,j}]_{i,j=1,\ldots,N}$ with $\mathbf{A} = \mathbf{X}'\mathbf{X}'^{\mathrm{T}} + \mathbf{Y}'\mathbf{Y}'^{\mathrm{T}}$, $\mathbf{X}' = [x_1', x_2', \ldots, x_N']^{\mathrm{T}}$, and $\mathbf{Y}' = [y_1', y_2', \ldots, y_N']^{\mathrm{T}}$. It should be noted that $\mathbf{A}$ is symmetric. Using matrix-vector notation we obtain the following compact form of the squared error

$$\xi^2 = \frac{\mathbf{G}^{\mathrm{T}}\mathbf{A}\mathbf{G}}{\mathbf{G}^{\mathrm{T}}\mathbf{1}\mathbf{G}}$$

from which the mean square error (MSE) simply follows

$$\mathsf{MSE} = \mathbb{E}\left[\frac{\mathbf{G}^{\mathrm{T}}\mathbf{A}\mathbf{G}}{\mathbf{G}^{\mathrm{T}}\mathbf{1}\mathbf{G}}\right] \qquad (6)$$

with $\mathbf{G} \sim \mathcal{N}(\boldsymbol{\mu}, \sigma_s^2\mathbf{I})$ and $\boldsymbol{\mu} = \mathbb{E}[\mathbf{G}]$. The vector $\boldsymbol{\mu}$ has elements $\mu_i = \mathbb{E}[G_i] = \mathbb{E}[P_i] - P_{\min}$.[1]

Note that the expression (6) is the first order moment of the ratio of quadratic forms in normal variables investigated in [15], [16]. In [16] it is possible to find the exact expression of expectation in the form of (6) by exploiting the moment generating function (MGF), i.e.,

$$\mathbb{E}\left[\frac{\mathbf{G}^{\mathrm{T}}\mathbf{A}\mathbf{G}}{\mathbf{G}^{\mathrm{T}}\mathbf{B}\mathbf{G}}\right] = \int_0^\infty \phi(0, -t)\left(\mathrm{Tr}(\mathbf{R}) + \tilde{\boldsymbol{\mu}}^{\mathrm{T}}\mathbf{R}\tilde{\boldsymbol{\mu}}\right) dt \qquad (7)$$

where

$$\begin{aligned}\phi(0, -t) = &[\det(\mathbf{I} + 2t\mathbf{B})]^{-1/2} \\ &\times \exp\left(\frac{1}{2}\left(\boldsymbol{\mu}^{\mathrm{T}}(\mathbf{I} + 2t\mathbf{B})^{-1}\boldsymbol{\mu} - \boldsymbol{\mu}^{\mathrm{T}}\boldsymbol{\mu}\right)\right)\end{aligned} \qquad (8)$$

is the joint MGF of the ratio terms, $\mathbf{R} = \mathbf{L}^{\mathrm{T}}\mathbf{A}\mathbf{L}$, $\tilde{\boldsymbol{\mu}} = \mathbf{L}^{\mathrm{T}}\boldsymbol{\mu}$, and $\mathbf{L}\mathbf{L}^{\mathrm{T}} = (\mathbf{I} + 2t\mathbf{B})^{-1}$.

In our case, the matrix $\mathbf{B}$ is equal to $\mathbf{1}$, hence the term $\mathbf{L}\mathbf{L}^{\mathrm{T}}$ can be written as $\mathbf{L}\mathbf{L}^{\mathrm{T}} = (\mathbf{I} + 2t\mathbf{1})^{-1} = \mathbf{C}(t)$ which in turn can be simplified to

$$\mathbf{C}(t) = \mathbf{I} - \frac{2t}{1 + 2nt}\mathbf{1}. \qquad (9)$$

Therefore

$$\begin{aligned}\mathrm{Tr}(\mathbf{R}) &= \mathrm{Tr}(\mathbf{L}^{\mathrm{T}}\mathbf{A}\mathbf{L}) = \mathrm{Tr}(\mathbf{A}\mathbf{L}\mathbf{L}^{\mathrm{T}}) = \mathrm{Tr}(\mathbf{A}\mathbf{C}(t)) \\ &= \mathrm{Tr}(\mathbf{A}) - \frac{2t}{1 + 2nt}\mathrm{Tr}(\mathbf{A}\mathbf{1})\end{aligned}$$

and

$$\begin{aligned}\tilde{\boldsymbol{\mu}}^{\mathrm{T}}\mathbf{R}\tilde{\boldsymbol{\mu}} &= \boldsymbol{\mu}^{\mathrm{T}}\mathbf{L}\mathbf{R}\mathbf{L}^{\mathrm{T}}\boldsymbol{\mu} = \boldsymbol{\mu}^{\mathrm{T}}\mathbf{L}\mathbf{L}^{\mathrm{T}}\mathbf{A}\mathbf{L}\mathbf{L}^{\mathrm{T}}\boldsymbol{\mu} \\ &= \boldsymbol{\mu}^{\mathrm{T}}\mathbf{M}(t)\boldsymbol{\mu}\end{aligned}$$

[1] We consider the case of i.i.d. shadowing although the more general case of correlated shadowing i.e., $\mathbf{G} \sim \mathcal{N}(\boldsymbol{\mu}, \boldsymbol{\Sigma})$, with $\boldsymbol{\Sigma}$ non-diagonal, can be handled as well.

$$\mathsf{MSE} = \int_0^\infty (1+2nt)^{-1/2} \exp\left(-\frac{t}{1+2nt}\boldsymbol{\mu}^{\mathrm{T}}\mathbf{1}\boldsymbol{\mu}\right) \times \left(\mathrm{Tr}(\mathbf{A}) + \boldsymbol{\mu}^{\mathrm{T}}\mathbf{A}\boldsymbol{\mu} - \frac{2t}{1+2nt}\mathrm{Tr}(\mathbf{A1}) - \frac{4t}{1+2nt}\boldsymbol{\mu}^{\mathrm{T}}\mathbf{A1}\boldsymbol{\mu} + \left(\frac{2t}{1+2nt}\right)^2 \boldsymbol{\mu}^{\mathrm{T}}\mathbf{1A1}\boldsymbol{\mu}\right) dt \tag{12}$$

where $\mathbf{M}(t) = \mathbf{C}(t)\mathbf{A}\mathbf{C}(t)$. Expanding $\mathbf{M}(t)$ we get

$$\mathbf{M}(t) = \mathbf{A} - \frac{2t}{1+2nt}\mathbf{A1} - \frac{2t}{1+2nt}\mathbf{1A} + \left(\frac{2t}{1+2nt}\right)^2 \mathbf{1A1}$$

from which

$$\begin{aligned}\boldsymbol{\mu}^{\mathrm{T}}\mathbf{M}(t)\boldsymbol{\mu} &= \boldsymbol{\mu}^{\mathrm{T}}\mathbf{A}\boldsymbol{\mu} - \frac{2t}{1+2nt}\boldsymbol{\mu}^{\mathrm{T}}\mathbf{A1}\boldsymbol{\mu} - \frac{2t}{1+2nt}\boldsymbol{\mu}^{\mathrm{T}}\mathbf{1A}\boldsymbol{\mu} \\ &\quad + \left(\frac{2t}{1+2nt}\right)^2 \boldsymbol{\mu}^{\mathrm{T}}\mathbf{1A1}\boldsymbol{\mu} \\ &\overset{(a)}{=} \boldsymbol{\mu}^{\mathrm{T}}\mathbf{A}\boldsymbol{\mu} - \frac{4t}{1+2nt}\boldsymbol{\mu}^{\mathrm{T}}\mathbf{A1}\boldsymbol{\mu} \\ &\quad + \left(\frac{2t}{1+2nt}\right)^2 \boldsymbol{\mu}^{\mathrm{T}}\mathbf{1A1}\boldsymbol{\mu}\end{aligned}$$

where (a) follows from the fact that $\boldsymbol{\mu}^{\mathrm{T}}\mathbf{A1}\boldsymbol{\mu} = \boldsymbol{\mu}^{\mathrm{T}}\mathbf{1A}\boldsymbol{\mu}$. Therefore, the second term of the integral (7) can be expressed as

$$\begin{aligned}\mathrm{Tr}(\mathbf{R}) + \tilde{\boldsymbol{\mu}}^{\mathrm{T}}\mathbf{R}\tilde{\boldsymbol{\mu}} &= \mathrm{Tr}(\mathbf{A}) + \boldsymbol{\mu}^{\mathrm{T}}\mathbf{A}\boldsymbol{\mu} \\ &\quad - \frac{2t}{1+2nt}\mathrm{Tr}(\mathbf{A1}) - \frac{4t}{1+2nt}\boldsymbol{\mu}^{\mathrm{T}}\mathbf{A1}\boldsymbol{\mu} \\ &\quad + \left(\frac{2t}{1+2nt}\right)^2 \boldsymbol{\mu}^{\mathrm{T}}\mathbf{1A1}\boldsymbol{\mu}. \end{aligned} \tag{10}$$

Now we simplify the joint MGF in (7)

$$\begin{aligned}\phi(0,-t) &= [\det(\mathbf{I}+2t\mathbf{1})]^{-1/2} \\ &\quad \times \exp\left(\frac{\boldsymbol{\mu}^{\mathrm{T}}(\mathbf{I}+2t\mathbf{1})^{-1}\boldsymbol{\mu}}{2} - \frac{\boldsymbol{\mu}^{\mathrm{T}}\boldsymbol{\mu}}{2}\right)\end{aligned}$$

noting that in our setting $\det(\mathbf{I}+2t\mathbf{1}) = 1+2nt$, obtaining

$$\phi(0,-t) = (1+2nt)^{-1/2}\exp\left(\frac{\boldsymbol{\mu}^{\mathrm{T}}\mathbf{C}(t)\boldsymbol{\mu}}{2} - \frac{\boldsymbol{\mu}^{\mathrm{T}}\boldsymbol{\mu}}{2}\right).$$

Expanding the terms in the exponential and using (9) we get

$$\begin{aligned}\frac{\boldsymbol{\mu}^{\mathrm{T}}\mathbf{C}(t)\boldsymbol{\mu}}{2} - \frac{\boldsymbol{\mu}^{\mathrm{T}}\boldsymbol{\mu}}{2} &= \frac{\boldsymbol{\mu}^{\mathrm{T}}\boldsymbol{\mu}}{2} - \frac{2t}{2(1+2nt)}\boldsymbol{\mu}^{\mathrm{T}}\mathbf{1}\boldsymbol{\mu} - \frac{\boldsymbol{\mu}^{\mathrm{T}}\boldsymbol{\mu}}{2} \\ &= -\frac{t}{1+2nt}\boldsymbol{\mu}^{\mathrm{T}}\mathbf{1}\boldsymbol{\mu}\end{aligned}$$

from which the final expression of the joint MGF appears as

$$\phi(0,-t) = (1+2nt)^{-1/2}\exp\left(-\frac{t}{1+2nt}\boldsymbol{\mu}^{\mathrm{T}}\mathbf{1}\boldsymbol{\mu}\right). \tag{11}$$

Substituting (10) and (11) into (7) we obtain the desired expression for the MSE (12) and consequently the RMSE in (5).

IV. Case Study Analysis

In this section, we analyze the methodology provided in Section III. In particular we compare analytical and simulation results of the RMSE of location estimation for random, but fixed, SU positions. The case study scenario is a square area with side $\mathcal{S} = 100\,\mathrm{m}$, with a PU transmit power $P_{\mathrm{t}} = 20\,\mathrm{dBW}$, shadowing parameter $\sigma_{\mathrm{s}} = 5.5\,\mathrm{dB}$ and $8\,\mathrm{dB}$, and path-loss exponent α between 3 and 4. Fig. 1 depicts the considered randomly distributed SUs and the PU located in three different positions: $L_{\mathrm{p}}^{\mathrm{A}} = (0\,\mathrm{m}, 0\,\mathrm{m})$, $L_{\mathrm{p}}^{\mathrm{B}} = (20\,\mathrm{m}, 0\,\mathrm{m})$ and $L_{\mathrm{p}}^{\mathrm{C}} = (40\,\mathrm{m}, 50\,\mathrm{m})$. To validate the analytical approach we used Monte-Carlo simulation with 1000000 runs.

Impact of PU location. In Fig. 2 we depict the WCL performance in terms of the RMSE of position estimation using the exact analysis and simulation results for the aforementioned PU locations, with $\alpha = 4$. There is an increase in the RMSE as the PU moves from the center at $L_{\mathrm{p}}^{\mathrm{A}}$ towards the edge of the area at $L_{\mathrm{p}}^{\mathrm{C}}$. This behavior is due to the nature of WCL which tends to be biased towards the center of the network, as was also observed through numerical simulations in [11], [12]. It is also evident that for the PU locations $L_{\mathrm{p}}^{\mathrm{B}}$ and $L_{\mathrm{p}}^{\mathrm{C}}$, the WCL does not benefit from increasing the number of SUs and as a result the localization performance remains almost constant when N increases from 120 to 250. The fluctuation in the RMSE for scenarios $L_{\mathrm{p}}^{\mathrm{B}}$ and $L_{\mathrm{p}}^{\mathrm{C}}$ with relatively low number of SUs is possibly due to the specific node locations, chosen randomly, in which the geometric configuration among SUs relative to the PU impacts the RMSE. However, for the case with the PU in the center of the area, increasing the nodes density improves the accuracy of the WCL.

Shadowing Analysis. We further analysed the WCL performance when varying σ_{s} between 4 dB and 10 dB, for $N = 240$ SUs and path-loss exponent $\alpha = 4$. As expected, the RMSE is not impacted by the variation of σ_{s}. This lack of dependency on σ_{s} is confirmed by (12).[2]

Path-loss Analysis. In Fig. 3 we show the impact the variation of the path-loss exponent α has on the RMSE, and we considered the following scenarios: PU locations $L_{\mathrm{p}}^{\mathrm{A}}$ and $L_{\mathrm{p}}^{\mathrm{B}}$, $\alpha = 3$ and 4, $\sigma_s = 5.5\,\mathrm{dB}$. Interestingly, the RMSE improves with an increase in α, as was observed numerically in [11]. Basically, increasing α in a way induces a node selection strategy which effectively reduces the impact of the SUs with low RSS on the location estimate [11], [12].

[2]On this point, we would like to remark that the RMSE provides localization performance in the average sense, hence a more complete analysis requires the statistical distribution of the two-dimensional error.

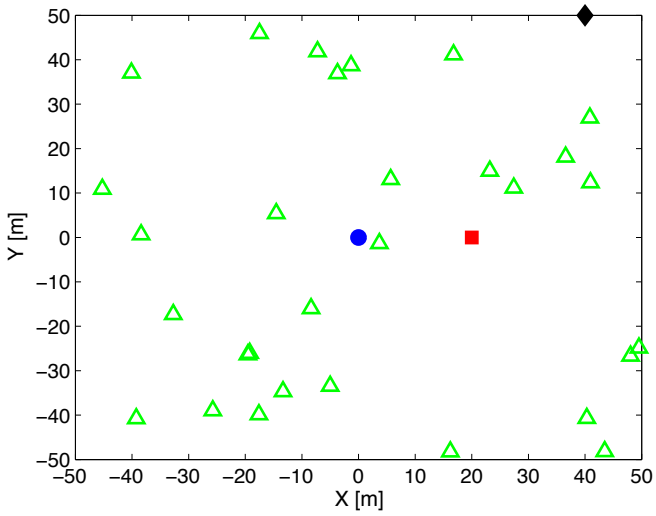

Fig. 1. The case study considered with randomly located SUs (triangles) and different PU positions: circle, square and diamond represent PU locations $L_{\mathrm{p}}^{\mathrm{A}}$, $L_{\mathrm{p}}^{\mathrm{B}}$ and $L_{\mathrm{p}}^{\mathrm{C}}$, respectively.

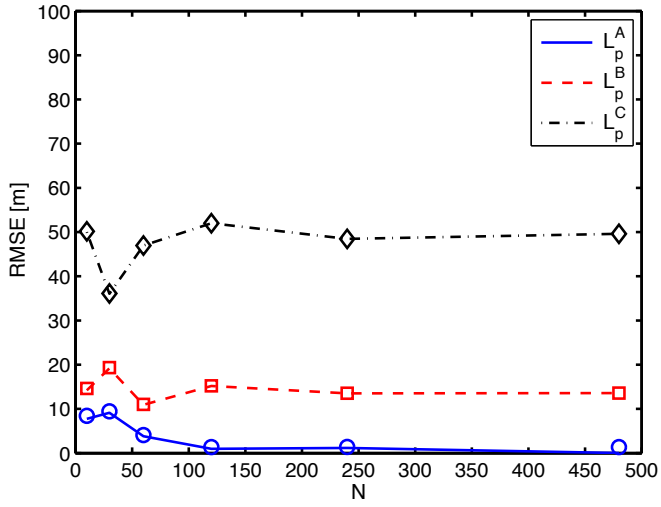

Fig. 2. RMSE of the two-dimensional position estimation as a function of the number of SU nodes, N, when the PU is located at $L_{\mathrm{p}}^{\mathrm{A}}$, $L_{\mathrm{p}}^{\mathrm{B}}$ and $L_{\mathrm{p}}^{\mathrm{C}}$. Lines and symbols refer to analytical and simulation results, respectively.

V. Conclusion

In this paper, we proposed a new analytical framework to calculate the exact performance of WCL in the presence of log-normal shadowing, based on results on the ratio of two quadratic forms in normal variables. In particular, we derived the expression for the RMSE of the two-dimensional localization error. A case study analysis was performed to evaluate the accuracy of the proposed methodology. Specifically, we analyzed the performance of WCL under varying PU location, path-loss exponent, number of SUs and their location. Numerical results confirm that the statistical framework is able to predict the performance of WCL capturing all the essential

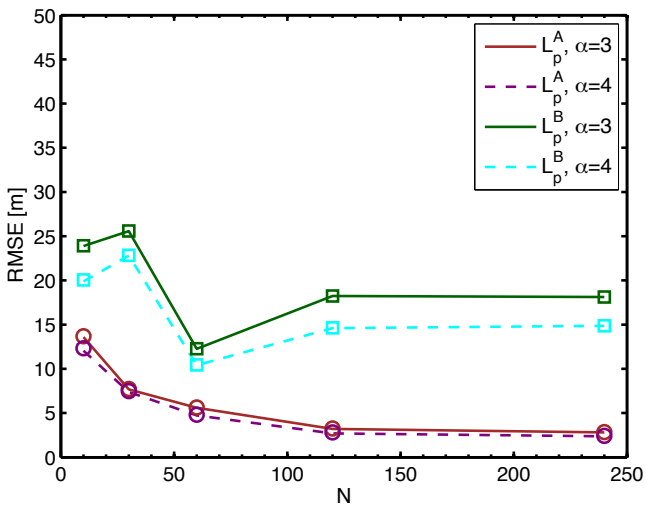

Fig. 3. RMSE of the two-dimensional position estimation as a function of the number of SU nodes, N, when the PU is located at $L_{\mathrm{p}}^{\mathrm{A}}$ and $L_{\mathrm{p}}^{\mathrm{B}}$, and for two different values of the path-loss exponent. Lines and symbols refer to analytical and simulation results, respectively.

aspects of propagation as well as CRs location. Future work will incorporate distance-dependent and correlated log-normal shadowing.

Acknowledgment

This work was supported in part by the European project EuroCPS (grant no. 644090) under the Horizon 2020 framework.

References

[1] K. Sithamparanathan and A. Giorgetti, *Cognitive Radio Techniques: Spectrum Sensing, Interference Mitigation and Localization*. Boston, USA: Artech House Publishers, Nov. 2012.

[2] A. Mariani, S. Kandeepan, and A. Giorgetti, "Periodic spectrum sensing with non-continuous primary user transmissions," *IEEE Trans. on Wireless Comm.*, vol. 14, no. 3, pp. 1636–1649, March 2015.

[3] S. Yarkan and H. Arslan, "Exploiting location awareness toward improved wireless system design in cognitive radio," *IEEE Comm. Mag.*, vol. 46, no. 1, pp. 128–136, January 2008.

[4] A. Conti, M. Guerra, D. Dardari, N. Decarli, and M. Z. Win, "Network experimentation for cooperative localization," *IEEE J. on Sel. Areas in Comm.*, vol. 30, no. 2, pp. 467–475, 2012.

[5] D. Dardari, A. Conti, U. Ferner, A. Giorgetti, and M. Z. Win, "Ranging with ultrawide bandwidth signals in multipath environments," *Proc. of the IEEE*, vol. 97, no. 2, pp. 404–426, 2009.

[6] M. Z. Win, A. Conti, S. Mazuelas, Y. Shen, W. M. Gifford, D. Dardari, and M. Chiani, "Network localization and navigation via cooperation," *IEEE Comm. Mag.*, vol. 49, no. 5, pp. 56–62, 2011.

[7] S. Bartoletti, W. Dai, A. Conti, and M. Z. Win, "A mathematical model for wideband ranging," *IEEE J. of Sel. Topics in Sig. Proc.*, vol. 9, no. 2, pp. 216–228, 2015.

[8] W. Dai, Y. Shen, and M. Z. Win, "Distributed power allocation for cooperative wireless network localization," *IEEE J. on Sel. Areas in Comm.*, vol. 33, no. 1, pp. 28–40, 2015.

[9] Y. Shen, W. Dai, and M. Z. Win, "Power optimization for network localization," *IEEE/ACM Trans. on Net.*, vol. 22, no. 4, pp. 1337–1350, 2014.

[10] J. Blumenthal, R. Grossmann, F. Golatowski, and D. Timmermann, "Weighted centroid localization in zigbee-based sensor networks," in *IEEE Int. Symp. on Intelligent Signal Proc. (WISP)*, 2007, pp. 1–6.

[11] A. Mariani, S. Kandeepan, A. Giorgetti, and M. Chiani, "Cooperative weighted centroid localization for cognitive radio networks," in *IEEE Int. Symp. on Comm. and Inf. Tech. (ISCIT)*, Gold Coast, Australia, Oct. 2012, pp. 459–464.

[12] K. Magowe, S. Kandeepan, A. Giorgetti, and X. Yu, "Constrained cluster based blind localization of primary user for cognitive radio networks," in *IEEE Int. Symp. on Pers., Indoor, and Mobile Radio Comm. (PIMRC)*, 2015, pp. 986–991.

[13] K. Magowe and S. Kandeepan, "Cooperative blind localization of primary user in a cognitive radio environment," in *IEEE Int. Conf. on Signal Proc. and Comm. Sys. (ICSPCS)*, 2014, pp. 1–8.

[14] J. Wang, P. Urriza, Y. Han, and D. Cabric, "Weighted centroid localization algorithm: theoretical analysis and distributed implementation," *IEEE Trans. on Wireless Comm.*, vol. 10, no. 10, pp. 3403–3413, 2011.

[15] A. Ullah, *Finite sample econometrics*. Oxford University Press, 2004.

[16] Y. Bao and R. Kan, "On the moments of ratios of quadratic forms in normal random variables," *J. of Multivariate Analysis*, vol. 117, pp. 229–245, 2015.

[17] S. Chaudhari and D. Cabric, "Cyclic weighted centroid localization for spectrally overlapped sources in cognitive radio networks," in *IEEE Global Comm. Conf. (Globecom)*, 2014, pp. 935–940.